



BOĞAZIÇI UNIVERSITY
School of Engineering - Department of Civil Engineering

**V. YERLİCİ - ENGINEERING AND
EDUCATION**

*A Volume Honoring
Prof. Dr. Vedat Yerlici*

EDITOR
GÜLAY AŞKAR ALTAY

May 22, 1997
İstanbul

Some Observations on the Nonclassical Behavior of Structures

M. Sayar, M. C. Demirel and A. R. Atılğan

Department of Civil Engineering and Polymer Research Center
Boğaziçi University, 80815 Bebek, İstanbul, Turkey

ABSTRACT

One-dimensional structures with finite number of repeat units are generated so as to analyze several nonclassical topics which has gained interest recently. These topics include but are not limited to the effect of distributed irregularities and point defects, the equilibrium dynamics of structural phase transitions, the environment-structure interactions, outcome of competitions ---which are between the environment and the perturbations caused by the functions of the structure--- on the structural response, especially structural noise and stochastic resonance applications, and the prediction of the long term behavior based upon the previous history of the time evolution. Each of these issues is discussed along with an example demonstrating the significance of the subject.

INTRODUCTION

Recently, in parallel with the technological advancements, number of studies dealing with the modeling of structural details and simulation of their intriguing behavior have increased. The main topics of interest include the effects of (i) irregularities present in the structure due to the manufacturing conditions (Benaroya, 1996; Sayar *et al.*, 1996), (ii) the surrounding environment on the long-term behavior (Amadei *et al.*, 1993; Baysal *et al.*, 1996; Demirel *et al.*, 1997), (iii) the tandem interaction between the surrounding environment and the loading which is the resultant of the function of the structure (Gang *et al.*, 1996; Austiman *et al.*, 1994; Rousset *et al.*, 1994). Any endeavor related with these nonclassical issues necessitates the utilization of efficient dynamical simulation techniques.

Molecular Dynamics (MD) simulations have been used extensively in different areas of mechanics (Ciccotti and Hoover, 1986; Hoover, 1991). MD technique solves Newton's equations of motion for each degree of freedom. However, the nature of the solution strategy may differ depending on the conserved quantities during the time evolution. In the absence of mass transfer, mainly, there are two different thermodynamical ensemble: microcanonical and canonical. In the microcanonical time evolution, dynamics of the system with finite number of degrees of freedom prevails on

constant energy surface. Therefore, the total energy of the system must be conserved each time step during the simulation. In the canonical time evolution, on the other hand, the system interacts with a thermal bath. Thus, in this case, the temperature of the system must be conserved. While the former technique is well suited for estimating the effects of disorder in the structure, the latter technique provides an enabling methodology for undertaking the effects of the surrounding media.

In this study, one-dimensional (1D) structures composed of finite number of substructures are investigated. The following nonclassical topics are undertaken: realization of structural vibrations due to irregularities embedded in the structure, structural motor and stochastic resonance phenomena caused by the combined effects of perturbations from noise and interactions with other systems, and the long term predictions by statistical simulations and reduced space integration algorithms.

COMPUTATIONAL MODELING

The generic configuration of the present study is the 1D structure with finite number of repeat units (substructures) as shown in Figure 1. The main ingredients of the system are the substrate energy and the kinetic energy for each DOF, and the interaction energy between the substructures. In the analysis of different nonclassical effects, miscellaneous degeneracies of total configurational energy are selected.

mechanical dynamics

The total energy of the system may be expressed in the following form

$$E = E_k + E_s + E_c \tag{1}$$

$$E_k = \sum_{i=1}^N \frac{1}{2} v_i^2 \quad E_s = \sum_{i=1}^N \left(\frac{1}{2} u_i^2 + \frac{1}{4} u_i^4 \right)$$

$$E_c = \sum_{i=1}^N \frac{1}{2} (u_i - u_{i-1})^2 + \frac{1}{4} (u_i - u_{i-1})^4$$

where E_k , E_s , and E_c denote the kinetic, substrate, and the coupling energy contributions, respectively, and E is the total energy. Here u_i is the displacement and v_i the velocity of each repeat unit from its equilibrium configuration. The equations of motion may be obtained as

$$\dot{u}_i = \frac{\partial E}{\partial v_i}$$

$$\dot{v}_i = - \frac{\partial E}{\partial u_i} \tag{2}$$

here overdot denotes differentiation with respect to time. The numerical integration of these equations may be referred to as microcanonical simulations provided that at each time step the total energy of the system is conserved.

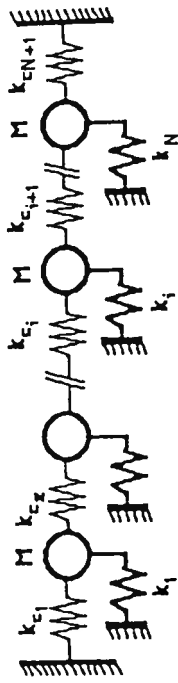


Figure 1. One-dimensional structure with N substructures. Here k_i represent the grounding stiffness of the each substructure, $k_{e,i}$ denotes the coupling stiffness between the substructures i and $i-1$, and M denotes the mass.

Canonical dynamics

If the system interacts with an environment of constant temperature, the coupling to the environment may be activated by introducing two additional degrees of freedom (Kusnezov *et al.*, 1990). The equations of motion in the extended space is

$$\dot{u}_i = v_i - \xi u_i^3$$

$$\dot{v}_i = - \frac{\partial E}{\partial u_i} - \zeta^3 v_i \tag{3}$$

$$\dot{\zeta} = \alpha \left(\sum_{i=1}^N v_i^2 - NT \right)$$

$$\dot{\xi} = \gamma \left(\sum_{i=1}^N u_i^3 \frac{\partial E}{\partial u_i} - 3T \sum_{i=1}^N u_i^2 \right)$$

Here the first two equations without ξ and ζ terms are the equations of motion of the original system. Therefore, ξ and ζ are the parameters which activates the coupling to the thermal bath. It is suggested that $\alpha = 1/T$ and $\gamma = 1/T^2$ be taken for optimal coupling conditions (Kusnezov *et al.*, 1990) during the numerical experiments.

Characterization of the time evolution

We express the time evolution of the configurational state of the system with N degrees of freedom by a trajectory matrix A as

$$A = [a_1, a_2, \dots, a_n] \tag{4}$$

Here the elements a_i ($1 \leq i \leq n$) are N -dimensional vectors characterizing the instantaneous configuration of the system. We use the singular value decomposition technique and decompose the $N \times n$ matrix A into the product of three matrices as

$$A = U S V^T \tag{5}$$

where S is an $N \times N$ diagonal matrix, the elements of which are the singular values of A . Here U is an $N \times N$ orthonormal matrix whose columns are the left singular vectors each

system relevant to the actual mechanism of motion. The columns of V are the corresponding right singular vectors. $U^T A$ gives the projections of the instantaneous configurations a_i along the singular directions.

ong term prediction

Suppose we have d zero (or close to zero) singular values obtained from the A matrix (eq. 4) of a mechanical system whose governing equations are in the form of $\ddot{x} = f(x)$. It may be shown that every holonomic constraint corresponds to a zero singular value of the trajectory matrix (Amadei *et al.*, 1993). The basis set spanning the $(N-d)$ dimensional null space of the trajectory matrix may be obtained from the columns of U' which is an $N \times (N-d)$ dimensional matrix satisfying $A = U' S' V'^T$. Here S' and V'^T are $(N-d) \times (N-d)$ and $(N-d) \times n$ dimensional matrices, respectively. The projection of the governing equations on the $(N-d)$ dimensional space may be readily accomplished in the following manner

$$\ddot{y} = U'^T f(x) = g(y) \quad (6)$$

where y is an $(N-d)$ -vector given by $y = U'^T x$. The projection matrix U' is customarily obtained as the Hessian matrix of the governing potential (Noor, 1981; Space *et al.*, 1993). The dimension $(N-d)$ of the solution space, which is a part of the configuration space that the trajectories actually explore, may be much smaller than that of configuration space (Amadei *et al.*, 1993; Baysal *et al.*, 1996). Thus, the time integration process may be performed more economically in the constraint-free $(N-d)$ dimensional space without destroying the essential mechanics of the motion.

A measure for structural irregularities

Let $f_j(t)$ be the amplitude of the i th substructure for the j th mode. For the linear system, $f_j(t)$ is the j th eigenvector of the matrix $(-\omega^2 M I + K)$ where ω^2 is the natural frequency, K is the conventional tridiagonal stiffness matrix of the system, and I is the identity matrix. For the nonlinear system, on the other hand, $f_j(t)$ is the j th column of the matrix U . It can be shown that columns of U coincide the eigenvectors inasmuch as the trajectories of the linearized system are employed in eq. 4. The mean, μ_j , the standard deviation, σ_j , and the kurtosis, κ_j , are defined as follows

$$\mu_j = \frac{\sum_{i=1}^N |f_j(t)|}{\sum_{i=1}^N |f_j(t)|}, \quad \sigma_j = \sqrt{\frac{\sum_{i=1}^N |f_j(t)|^2}{\sum_{i=1}^N |f_j(t)|} - \left(\frac{\mu_j}{\sigma_j}\right)^2}, \quad \kappa_j = \frac{\sum_{i=1}^N |f_j(t)|^4}{\left(\sum_{i=1}^N |f_j(t)|\right)^2} \quad (7)$$

We then define the localization of the j th mode as the difference in the kurtosis

$$L_j = \kappa_j(\text{disordered}) - \kappa_j(\text{perfect}) \quad (8)$$

CALCULATIONS AND RESULTS

The numerical integration is performed on the constant energy surface of the configurational space or on the extended space whenever the coupling to the environment is switched on. Thus at each time step the total energy of the (extended) system is preserved. Bulirsch-Stoer method (Press *et al.*, 1992) is utilized which conserves the energy upto the single precision machine accuracy. In what follows, results of the numerical simulations for different nonclassical effects are furnished.

Effect of structural irregularities

The model structure consists of 16 repeat units. Both ends of the chain are fixed. Considering the operating potentials given by eq. 1, for the linear case, we pick up only harmonic terms both in the substrate and in the coupling potentials; and take into account additionally the fourth order contribution in the coupling potential for the nonlinear case. In order to demonstrate strong localization, we set the grounding stiffness and the mass to unity, and the coupling stiffness to 0.01. The ratio σ_k/k_c is defined so as to measure the degree of randomness. Here σ_k is the standard deviation and the ratio is taken to be 0.213. The time evolution of the nonlinear system is obtained by numerically integrating eq. 2; and eqs 7 and 8 are employed so as to calculate the localization. It is seen in Figure 2 that the localization is observed both in the lower and in the higher modes for the linear system which is represented by the dashed line. The additional quartic intrastructural potential removes the localization from the lower modes as observed by the solid line. This is of critical importance since it is always desirable to eliminate high-amplitude displacements which are associated with lower modes.

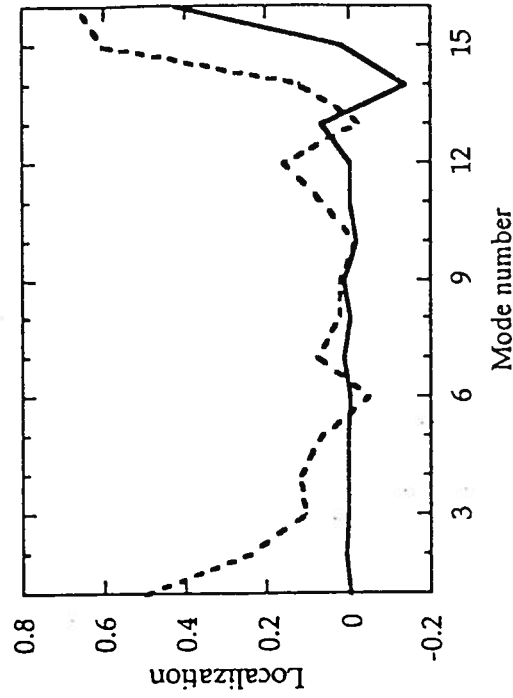


Figure 2. Kurtosis difference of the disordered configuration from those of the perfect for each mode (Eq. 7). Dashed and solid lines denote the linear and nonlinear configurations, respectively.

mulation of a point defect

We simulate the dynamics of the defect zone which is due to the presence of an edge dislocation (Askar, 1986). This zone is shown schematically in Figure 3(a) wherein substructures are designated by filled circles which are placed at the local maxima of the substrate potential that is a symmetric double well. The minima of this potential are the point where the empty circles are placed. In Figure 3(b), the displacements for the unrelaxed configuration and the relaxed configuration calculated using statics are

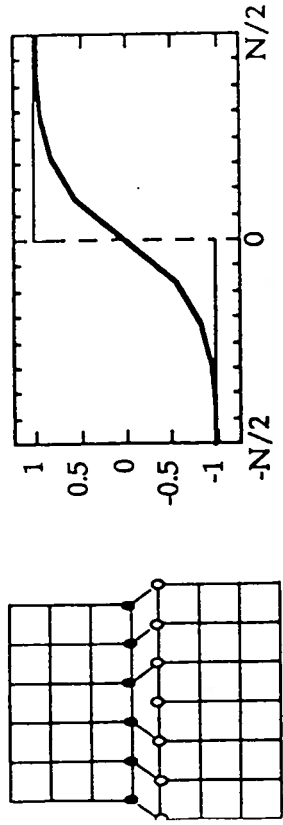


Figure 3. (a) Schematic view of the defect zone circumvented by the filled and the empty circles, (b) unrelaxed (thin line) and the relaxed displacement fields (thick line).

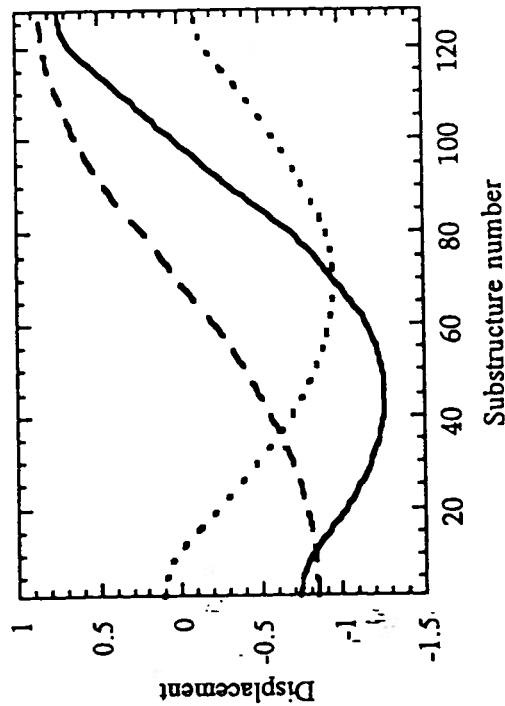


Figure 4. First two singular modes of the structure which determine the characteristic movement of the kink between the end points. Dashed and dotted lines denote the projection of the motion along the first and the second singular mode, respectively; the solid line is the superposition of the two.

associated with the thin straight lines and the thicker solid line, respectively. While the nonequilibrium displacement field exhibits a jump where the defect was initially present, the static equilibrium display a kink shape. The dynamical evolution of the unrelaxed to the relaxed configuration and the thermal fluctuations around the equilibrium may be simulated by the canonical dynamics. In this example, 128 substructures (filled circles) are considered. Figure 4 demonstrate that superposition of the first and the second singular modes denoted by the solid line characterizes well the dynamical equilibrium of the defect. While the first singular mode (dashed lines) preserves its equilibrium shape adjusting only its magnitude, the second singular mode by itself reconstructs the motion for the center of the defect (dotted lines).

Solitary waves

Time evolutions for displacements of the structure with 128 units are obtained by numerically integrating eq. 3. The operating potentials in this case are the same as the point defect analysis; the boundary conditions are different, however. In this example, both ends of the chain is free. During the computer experiments, total time evolution is divided into two parts: equilibration and simulation. The equilibration time for temperatures $1/T < 6$ is 10^3 time steps; however, for lower temperatures, it is 10^4 time steps. The simulation time for the range $1/T < 1/6$ is 9×10^3 time steps; for lower ranges, it is 9×10^4 time steps. A scaling law at low temperatures is related to the variation of the spatial correlation length with respect to the temperature. The scaling law involving the correlation length of the solitary wave may be defined by

$$C(x) = \langle u(0)u(x) \rangle \sim e^{-x/\lambda} \tag{9}$$

where λ is called the correlation length for which a theoretical prediction was obtained by Krumhansl and Schrieffer (1975) as $\lambda = (1/4) (\pi/3)^{1/2} (T/E)^{1/2} e E/T$. The variation

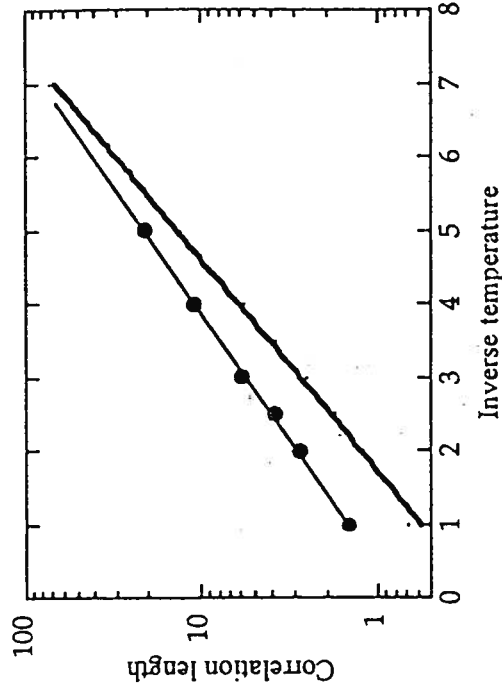


Figure 5. Scaling of the spatial correlation length with $1/T$. The thick solid line is the low temperature theoretical estimation (eq. 9), bullets are obtained numerically.

f the correlation length with respect to the temperature is shown in Figure 5. The thick solid line indicates the results obtained by eq. 9; the bullets are found by numerical experiments for different temperatures. The thinner solid line is used to guide the eye or the scaling law obtained computationally. Similar observations are also made by Alexander and Habib (1993) via Brownian dynamics simulations. It may be recognized that the slopes of the two curves are quite different; and the two curves may intersect at higher temperatures.

Effect of surrounding environment

The model structure is composed of 16 substructures. One end of the chain is fixed, the other is free. In this case, we consider only the coupling potential with harmonic and quartic terms; effect of substrate potential is not considered. This model is usually referred to as the Fermi-Pasta-Ulam (FPU) chain (Demirel *et al.*, 1997). The normalized single point probability distribution function of the free-end displacement u_N is shown in Figure 6. The dashed lines are obtained by numerically integrating eq. 10, the solid line is obtained theoretically by employing the saddle point approximation to the following integral in the infinite domain: $\int e^{-E(u)} du_1 du_2 \dots du_{N-1}$.

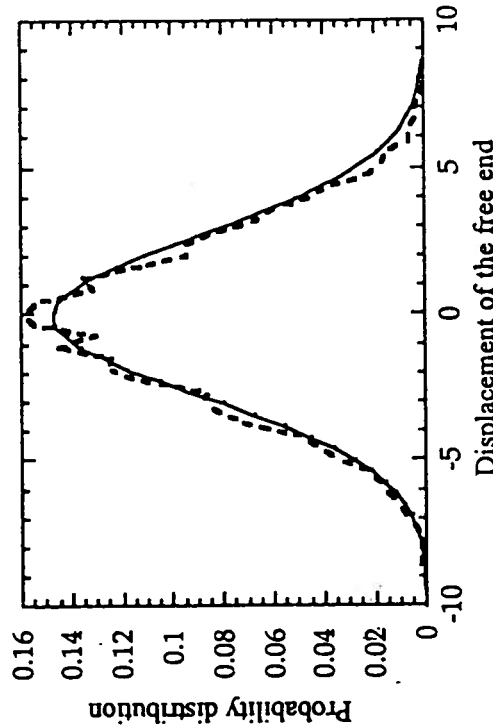


Figure 6. Probability density distribution for the end point displacement of the FPU chain. Solid line denote the theoretical predictions and dashed lines are obtained from numerical experiments.

Structural motor

It has been shown that structures which possess spatial asymmetry act as pumps in the presence of dissipation alone, without the need for macroscopic forces or temperature differences to drive a motion. Such behavior was demonstrated experimentally by Rousselet *et al.* (1994) and shown theoretically for the case in which particles subjected to an asymmetric periodic potential can display net directional

motion even if the space-average force is zero (Austiman and Bier, 1994). Stemming from these, we have studied the response of a 1D structure with 16 repeat units each of which is subjected to a symmetric substrate potential in the form of $V(u) = u_1^2 (u_1 - 1)^2 (u_1 + b)^2$. The communication between the substructures are achieved by a harmonic potential. Asymmetry in the potential is achieved by varying the parameter b periodically in time as $b = 1 + \sin 5t$. During the simulations, the temperature of the surrounding environment is held constant ($T = 1$) and no additional forces are considered. The time evolution of the displacements are recorded for 10^4 time steps. The probability distribution for the displacement of the free end is shown in Figure 7. The symmetry in the distribution is broken due to the perturbed potential and one state of the system cannot be explored anymore. Turning on and off the perturbations repeatedly in time, a directional motion may then be observed.

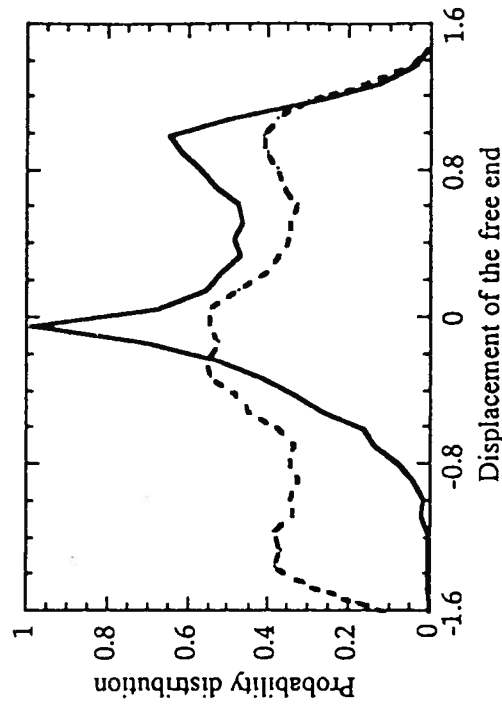


Figure 7. Probability distribution for the displacement of the free end. The dotted and the solid lines correspond to the displacement distributions obtained from the unperturbed and the perturbed potentials, respectively.

Stochastic resonance

It has been shown that a weak periodic signal can be amplified by the addition of external noise and this phenomenon is referred to as stochastic resonance (Dykman *et al.*, 1993; see also other references in the same issue). The response may be expressed in terms of the spectral density of displacements which is the square of the Fourier transform of the displacement fluctuations. Analytical calculations may be carried out in closed form if the linear response theory is employed which may not be sufficient depending on the type of nonlinearity (Dykman *et al.*, 1993). Here we consider a single DOF system which is coupled to heat bath that provides a continuous perturbation to the structure. The operating potential is a symmetric double well. A harmonic time dependent force ($a \cos \omega t$) with the amplitude of $a = 0.1$ and the frequency $\omega = 0.0695$ is applied to the system. In Figure 8, bath temperature is normalized by ΔU which is the

ference between the maximum and the local minimum of the substrate potential. The power spectrum is normalized by the amplitude of the force. The behavior exhibited in the figure is typically observed in practical applications (for instance, Figure 1 of Y'nan *et al.*, 1993; note especially that the fluctuating trend rather than a smooth decay after the peak in the amplitude spectrum is present in the measurements).

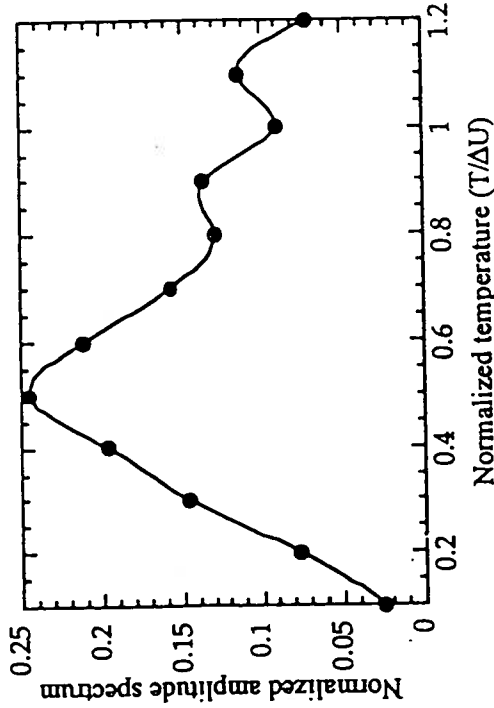


Figure 8. The ratio of the bath temperature to the breath of the substrate potential is the ratio spectral density of displacement fluctuations to the amplitude of the force. The filled circles are the calculated values, the solid line is obtained by interpolation.

Long-term predictions

We reconsider the FPU chain with 16 repeat units. The time evolution for the displacements are obtained for 10^4 time steps. It is found that only six of the sixteen singular values contribute to the essential mechanism of the motion. With the aid of this data ($d = 10$), we would like to predict the next 10^4 time steps using eqs. 4-6 in the six dimensional, reduced space. Determination of the duration time for the initial evolution for the trajectory matrix is of critical importance. The point-wise predictions calculated using the projection method start diverging from those calculated in the configurational space with the original equations after a short time. Thus, predictions of averaged quantities, such as mean and moments of the probability distributions of fluctuations, may be meaningful to predict for long-term analyses. In Figure 9, the probability distribution of the averaged displacement of two substructures located at the center are shown. The dashed lines are calculated by using the projection algorithm in the six dimensional space. They turn out to be a good approximation to the full space integrations (solid line).

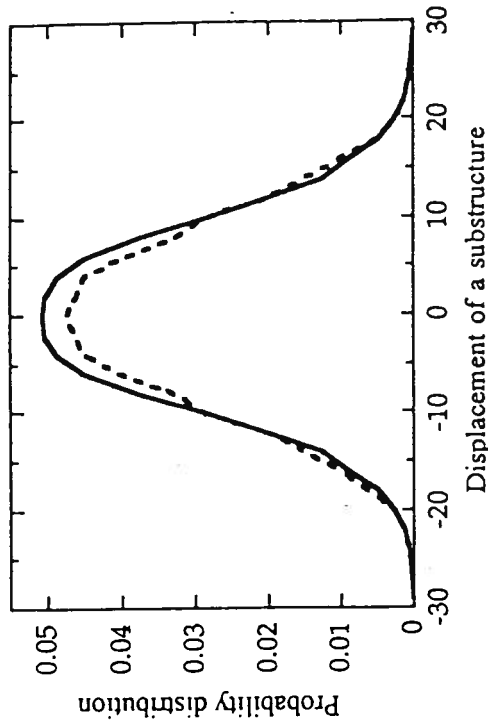


Figure 9. Probability distribution for the averaged displacement of two substructures located at the center. The solid and the dashed curves are obtained using 16 dimensional configurational space and six dimensional constraint-free reduced space, respectively.

CONCLUDING REMARKS

The main conclusions of the present study may be stated as follows: (i) The nonlinear interactions between the substructures remove the localization of the low-frequency modes observed in the linear case, (ii) first two singular modes of the motion created by 128 substructures surrounding the point defect are capable of producing the free-floating of the defect manifested in the kink shape, (iii) the numerical simulations based upon the canonical dynamics of the solitary waves indicate that the correlation length scales with the bath temperature and agrees with the theoretical predictions at the low temperature limit, (iv) the single point probability distributions calculated by the canonical dynamics method agree well with the theoretical estimations, (v) switching on and off perturbations to any symmetrical potential, one can generate a biased, directional motion for which an original state of the system cannot be explored; this is detected by the probability distributions of the displacements, (vi) the combination of the periodic driving force acting on the structure and the interaction of the structure with the surrounding environment can modulate the probabilities and can generate high amplitude thermal fluctuations, (vii) for predicting some averaged quantities, such as distributions of fluctuations, the integration of the equations of motion may be accomplished in a reduced dimensional space which is obtained solely by a limited time evolution of the full configuration.

Acknowledgments

Partial support is provided by the Bogazici University Research Funds Project No 96A0430 and The Boeing Company Project No PO FR-513570-07LLN.

REFERENCES

- exander, F. J., and Habib, S., (1993), "Statistical mechanics of kinks in 1+1 dimensions," *Physical Review Letters*, 71 (7), 955 – 958.
- nadei, A., Linssen, A. B. M., and Berendsen, H. J. C., (1993), "Essential dynamics proteins," *Proteins*, 17, 412 – 425.
- kar, A., (1986), *Lattice Dynamical Foundations of Continuum Theories*, World Scientific Publishing Co., Singapore.
- istiman, R. F., and Bier, M., (1994), "Fluctuation driven ratchets: Molecular motors," *Physical Review Letters*, 72, 1766 – 1769.
- ysal C., Atilgan A. R., Erman B., and Bahar I., (1995), "Coupling between different modes in local chain dynamics: A modal correlation analysis," *J. Chem. Soc. Faraday Trans.*, 91 (16), 2483 – 2490.
- aysal C., Atilgan A. R., Erman B., and Bahar I., (1996), "A molecular dynamics study of the coupling between the librational motions and isomeric jumps in chain molecules," *Macromolecules*, 29 (6), 2510 – 2514.
- enaroya, H., Ed., (1996), "Localization and effects of irregularities in structures," *Applied Mechanics Reviews*, 49 (2), 57 – 135.
- iccotti, G., and Hoover, W. G., Eds., (1986), *Molecular-Dynamics Simulation of Statistical-Mechanical Systems*, North-Holland, Amsterdam.
- emirel, M. C., Sayar, M., and Atilgan, A. R., (1997), "Statistical mechanics of Fermi-asta-Ulam chains with the canonical ensemble," *Physical Review E*, 55 (3), 55 – 58.
- ykman, M. I., Luchinsky, D. G., Mannella, R., McClintock, P. V. E., Stein, N. D., and Stocks, N. G., (1992), "Stochastic resonance: Linear response and giant nonlinearity," *Journal of Statistical Physics*, 70 (1/2), 463 – 478.
- iang, H., Daffertshofer, A., and Haken, H., (1996), "Diffusion of periodically forced brownian particles moving in space-periodic potentials," *Physical Review Letters*, 76 (26), 4874 – 4877.
- hoover, W. G., (1991), *Computational Statistical Mechanics*, Elsevier, Amsterdam.
- rumhansl, J.A., and Schrieffer, J.R., (1975), "Dynamics and statistical mechanics of a one-dimensional model Hamiltonian for structural phase transitions," *Physical Review* 3, 11 (9), 3535 – 3545.
- cusnezov, D., Bulgac, A., and Bauer, W., (1990), "Canonical ensembles from chaos," *Annals of Physics*, 204, 155 – 185.
- Noor, A. K., (1981), "Recent advances in reduction methods for nonlinear problems," *Press*, W. H., Teukolsky, S. A., Vetterling, W. T., and Flannery, B. P., (1992), *Numerical Recipes*, Second Edition, Cambridge University Press.
- Rousselet J., Salome L., Ajdari A., and Prost J., (1994), "Directional motion of Brownian particles induced by a periodic asymmetric potential," *Nature*, 370, 446 – 448.
- Sayar, M., Demirel, M. C., and Atilgan, A. R., (1996), "Dynamics of one-dimensional structures with designed-in disorder," *Proceedings of the 20th Congress of the International Council of the Aeronautical Sciences*, September 8 – 13, Sorrento, Italy, Vol. 2, 1418 – 1425.
- Space B., Rabitz, H., and Askar, A., (1993), "Long time scale molecular dynamics subspace integration method applied to anharmonic crystals and glasses," *J. Chem. Phys.*, 99, 9070 – 9079.

Future Transportation Fuels: The Case for Hydrogen W. D. Van Vorsi	117	Rubberlike Elasticity B. Erman
An Engineering Concept in Atomic Physics: Quantum Fluid Dynamics (QFD) A. Askar and F. S. Mayor	125	Effect of Compaction Energy on Hydraulic Conductivity of Lime Stabilized Clays E. Güler and I. Sargin
Instructure Spectra from Ground Spectra T. S. Atalık	135	Reconciling Engineering Research and Educational Activities: A Case Study E. Inclmen
Seismic Behavior of Precast Frames U. Ersoy	151	Computer Aided Concrete Mixture Design with the Prediction of Creep and Shrinkage T. Özturan and M. Arkan
An Experimental Study on Shear Carrying Capacity of Columns under Combined Bending, Shear, and Axial Loading M. Gerçek	159	Some Observations on the Nonclassical Behavior of Structures M. Sayar, M. C. Demirel and A. R. Atilgan
Midbroken Reinforced Concrete Shear Frames Due to Earthquakes H. U. Köyüoğlu, A. Ş. Çakmak and S. R. K. Nielsen	169	The Effective Rigidity of a Coupled Shear Wall S. S. Tezcan and Z. D. Kaya
The Golden Horn: Its Formation, Deterioration and Hopes for Rehabilitation K. Özyayın and M. Yıldırım	195	Beam Equations for Motions of Thermoelastic Materials G. Aşkar Altay and M. C. Dökmeci
Risk Metric: A Fire Insurance Decision Tool S. G. Velioglu and C. Gölpınar	211	
Self Strain of a Vertical Spring/Column An Exact Calculation R. Ö. Akyüz	223	
Algebraic Approach to the Calculation of Lyapunov Exponents I. Bırol and A. Hacınlıyan	227	
Clean Separation Technologies for Chemical Industries Ö. Hortacısu	237	
Removal of Petroleum and Petroleum Products by Dispersants in the Marine Environment G. Kocasoy and F. Borak	249	
Returns to Scale and Rate of Technical Change in Turkish Cement Industry S. Özmucur	265	
Effect of Pressure on Settling of Anaerobic Sludge K. Curi and M. Albukrek	275	
Flexible Earth Retaining Structures - Soil Nailing H. T. Durgunoğlu, H. F. Kulaç and C. G. Olgun	287	